2026 IEEE/SICE International Symposium on System Integration (SII)
January 11-14, 2026. Cancún, México

# Personal Space Toward Human-like and Non-human-like Robots: Effects of Robot Appearance and Likability

Rio Taguchi[1], Kaoruko Shinkawa[1], and Yoshihiro Nakata[1]

*Abstract*— **In this study, we investigated how robot appearance—human-like versus non-human-like—affects personal space during direct robot approaches from eight directions and examined the relationship between personal space and perceived likability. Twenty-three Japanese male participants participated in the experiment. The participants remained stationary while each robot approached from different directions (0°–315° in 45° increments), and the distance at which discomfort was perceived was recorded as the personal space threshold. Likability was assessed via a questionnaire. Across all conditions, a consistent negative correlation was observed between likability and personal space: participants who rated the robot more favorably tended to allow it to approach them more closely. No significant differences in personal space or likability were found between the two appearance conditions. However, the Human-like condition showed an almost circular personal space shape with an approximate radius of 1.35 m, slightly extended in its rear part, whereas the Non-human-like condition tended to have a personal space shape with a larger front and smaller rear parts. These results indicate that likability is closely associated with interpersonal distance regulation and suggest that manipulating perceived likability may serve as an effective strategy for managing personal space in service and interactive robot contexts. These findings may inform robot design approaches aimed at maintaining socially comfortable distances and improving overall user acceptance.**

## I. INTRODUCTION

With the use of robots expanding to tasks such as serving food, guiding, and cleaning, robots that move closer to people are being introduced [1]. In such scenarios, understanding the psychological impact of a robot's appearance and behavior on humans is expected to provide fundamental insights that contribute to the design of smooth human–robot interactions.

In Human–Robot Interaction (HRI) impression evaluations, self-report methods such as questionnaires and rating scales are primarily used. Zimmerman et al. [2] reviewed studies presented at the Association for Computing Machinery (ACM)/Institute of Electrical and Electronics Engineers (IEEE) International Conference on Human–Robot Interaction and the IEEE International Symposium on Robot and Human Interactive Communication from 2015 to 2021. They pointed out that many of these studies used custom-designed questionnaires, indicating a widespread reliance on self-report-based survey methods.

*This work was supported by JST (Moonshot R&D) Grant Number (JPMJMS2011).

[1]Rio Taguchi, Kaoruko Shinkawa, and Yoshihiro Nakata are with the Department of Mechanical and Intelligent Systems Engineering, Graduate School of Informatics and Engineering, The University of Electro-Communications, Chofu, Tokyo, 182-8585, Japan t2210380@gl.cc.uec.ac.jp, kshinkawa@uec.ac.jp, ynakata@uec.ac.jp

In this study, we focus on personal space as an evaluation metric to complement subjective impressions. Personal space refers to the psychological distance unconsciously maintained in response to the approach of others. Hall classified it into four zones: intimate, personal, social, and public distance [3]. This concept is not only used to understand spatial behavior in interpersonal situations but has also been applied in HRI as an indicator of how close humans allow robots to approach them [4], [5]. While questionnaires and rating scales rely on linguistic expressions and conscious judgment, personal space is characterized by the manifestation of unconscious judgments through behavior. Although the stopping point is based on participants' subjective judgment, it is manifested through measurable physical distances, thus providing a behavioral complement to purely linguistic self-reports.

Hecht et al. investigated personal space and likability when a person approached either another person or a mannequin [6]. The results show that the personal space maintained around the mannequin was significantly larger than that around a person ($p < 0.01$), and the mannequin was rated lower in likability than a human. Lehmann et al. conducted a study on personal space using the small humanoid robot "Nao" [7]. They found that when a person walked past the humanoid, the average distance maintained between humans and the robot was approximately 0.48 m. This value corresponded to the boundary of human-sized personal space rather than a boundary proportional to the robot's physical size, suggesting that personal space is not necessarily reduced solely due to a robot's small stature. Most existing studies have focused on situations where a human approaches another entity. In contrast, in real-world HRI scenarios, robots often approach humans, yet such cases have remained relatively underexplored.

Meanwhile, with the growing deployment of social robots in real-world applications, situations in which robots approach humans more closely are becoming common. Some studies have investigated human responses to these approaching behaviors [8], [9]; however, to the best of our knowledge, no prior study has investigated the concept of personal space in the context of a mobile android, i.e., robot with human-like appearance actively approaching a person. Although mobile androids such as "HRP-4C" [10], the "EveR" series [11], and "ibuki" [12] exist, no evaluations of personal space using these platforms have been reported.

In this study, we conducted an experiment using an android with mobility called "Yui" [13], in which the robot approached stationary participants from multiple directions

978-1-6654-5784-2/26/$31.00 ©2026 IEEE

under two appearance conditions. In the Human-like condition, the robot was equipped with a human-like head and dressed in clothing to enhance its human resemblance; in contrast, in the Non-human-like condition, the head was replaced with a mechanical-looking version, and the body was exposed to reveal its mechanical structure. The study aims to examine how variations in the degree of human-likeness in robot appearance influence the size of personal space during approach and to explore the relationship between appearance and perceived likability toward the robot.

The contributions of this study are as follows:

1) Developed an experimental system with a mobile android capable of approaching participants, enabling precise measurement of personal space
2) Quantified the size and shape of personal space under two distinct appearance conditions: human-like and non-human-like
3) Identified relationships between appearance-induced differences in personal space and subjective likability toward the robot

## II. ROBOT SYSTEM

This section provides an overview and describes the operational specifications of the robot system used in the experiment. Two appearance conditions were implemented to manipulate the degree of human-likeness: non-human-like and human-like.

### A. Overview of the Robot Platform

*1) Mechanical design:* We developed the wheeled mobile android Yui, shown in Fig. 1, and used it as the experimental platform. Yui is a 1.2-m-tall, battery-powered robot.

The upper body is equipped with a head capable of facial expressions and gaze movements [13]. The head incorporates 15 motors that drive 22 actuation points. As shown in Fig. 2, the rest of the upper body has three degrees of freedom (DOF) in the neck, three DOF in the waist, and seven DOF in each arm, allowing for human-like upper-body motions.

The lower body consists of a differential two-wheeled base supported by four caster wheels, enabling straight-line and turning movements. Additionally, it has one DOF for knee flexion. The joints corresponding to the ankles, knees, and waist are mechanically linked so that bending the knees alone keeps the upper body level. However, because the waist also has its own DOF, the upper body posture can be actively adjusted when necessary.

*2) Electrical system:* Each joint of the body is equipped with absolute encoders (magnetic encoders or potentiometers), which are connected via motor driver circuits to the control computer (UM790 Pro, 64 GB RAM, MINISFORUM) mounted on the mobile base. Power is supplied from a single battery ($LiFePO_4$, 24 V, 60 Ah) installed within the base.

*3) Control framework:* Each joint of the robot is angle-controlled to accept and adhere to command values issued by the control computer. The control computer runs on a Windows operating system and is responsible for managing the overall control of the robot. During the experiment, the robot's joint angles were controlled based on predefined time-series profiles assigned to each joint.

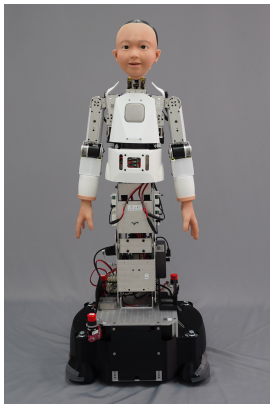

Fig. 1: Android "Yui," a child-sized, 1.2-m-tall mobile android platform.

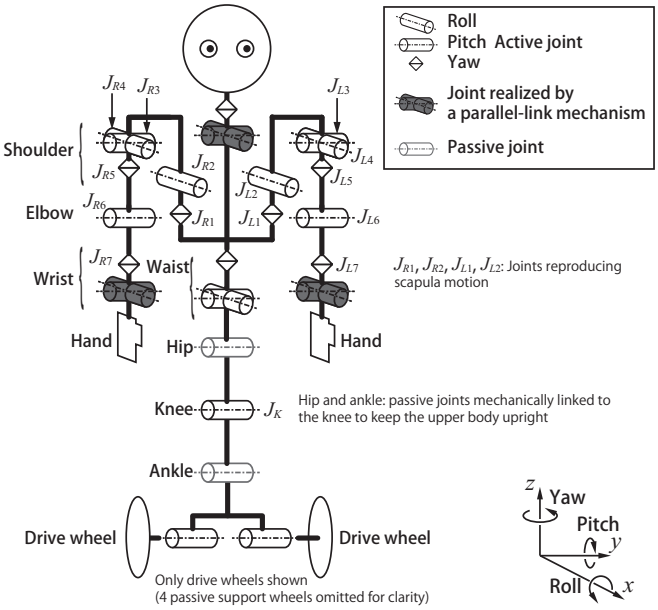


Fig. 2: Kinematic structure of android Yui, showing active and passive joints relevant to the experiment. Note that the wrist (roll and pitch) and hand were not motorized for this experiment.

### B. Motion Specifications

During the experiment, the robot was controlled to move straight toward the participant at a constant speed. Specifically, identical speed commands were given to both wheels, and speed control was applied to maintain a velocity of 0.34 m/s, except during the acceleration and deceleration phases. The wheel acceleration and deceleration in this experiment were both set to 0.131 $m/s^2$. As floor conditions could potentially cause deviations in the robot's path, wooden guides were installed on the floor along both sides of the robot's base, physically constraining its movement and ensuring that it maintained a consistent direction.

TABLE I: Joint Motion Profile Parameters

| $\theta$ | $A$ | $f$ | $\alpha$ | $\overline{\theta}$ |
|---|---|---|---|---|
| Right shoulder pitch $J_{R3}$ [°] | 13.4 | 0.575 | $\pi$ | -7.05 |
| Left shoulder pitch $J_{L3}$ [°] | 13.4 | 0.575 | 0 | -7.05 |
| Right elbow pitch $J_{R6}$ [°] | 5.47 | 0.575 | $\pi$ | -14.3 |
| Left elbow pitch $J_{L6}$ [°] | 5.47 | 0.575 | 0 | -14.3 |

During its motion along a straight-path, the robot executed movements designed to emulate human walking. Specifically, within a single walking motion cycle, the shoulders completed one full back-and-forth swing, while the knees flexed and extended twice, creating coordinated, gait-like motion.

To realize the motions mentioned above, the shoulder pitch joints ($J_{R3}, J_{L3}$), elbow pitch joints ($J_{R6}, J_{L6}$), and knee joint ($J_K$) were used, as shown in Fig. 2. $J_R$ denotes right, $J_L$ denotes left, and $J_K$ refers to the knee joint. From the initial posture shown in Fig. 2, the robot was operated by assigning target angles to these joints, whereas the motion of the other joints was constrained. The joint motion of the shoulder joints and elbow joints was determined using (1). According to this equation, the target angles for the shoulder and elbow joints were calculated based on $\theta$, and the target angles were applied to each motor. In the equation, $A$ denotes the angular amplitude, $t$ represents the elapsed time since the onset of motion, $f$ represents the oscillation frequency, $\alpha$ is the phase difference set to 0 or $\pi$ depending on whether it corresponds to the right or left side of the body, and $\overline{\theta}$ indicates the baseline angle. The parameters utilized are summarized in Table I.

$$\theta(t) = A\cos(2\pi t f + \alpha) + \overline{\theta}. \tag{1}$$

Subsequently, the targeted vertical oscillation was defined as follows. Beginning from full knee extension, where the upper and lower knee links are collinear, the upper body oscillated vertically at 1.15 Hz with a peak-to-peak amplitude of 32.3 mm, centered 16.15 mm below the initial posture—that is, the motion ranged from 0 mm to 32.3 mm below the initial level—with the vertical displacement $h$ given by (2).

$$h(t) = -16.15\{\cos(2.3\pi t + \frac{\pi}{2}) + 1\}. \tag{2}$$

To implement this motion, the motor actuating the knee joint was provided with a target vertical position defined by (2); this value was then converted to the corresponding knee-joint angle using (3) and applied as the target angle ($\theta_K$).

$$\theta_K = \arccos(1 + \frac{h}{2L}). \tag{3}$$

Here, 0° corresponds to full knee extension, when the upper and lower knee links are collinear. In these equations, $L = 190$ mm represents the equal lengths of the upper and lower knee links. Owing to motor limitations, the actual amplitude achieved was smaller than the target; however, since the primary aim of this experiment was to assess the robot's appearance, this reduction in knee-joint amplitude was considered negligible, and the experiment proceeded without additional adjustment.

(a) Non-human-like robot. (b) Human-like robot.

Fig. 3: Two types of robots with different appearances.

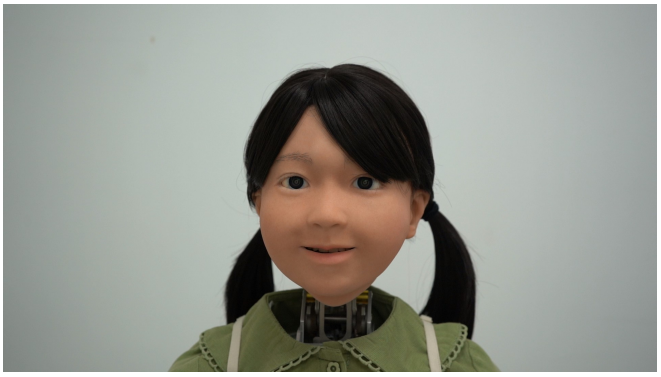

Fig. 4: Facial expression of the human-like robot during the experiment.

To quantify personal space, the robot's travel distance was calculated from the cumulative rotation measured by the wheel encoders and the known wheel diameter (0.14 m). The accuracy of the distance calculated from the encoders was verified in advance. Based on values measured with a tape measure, 10 trials were conducted in which the robot traveled 3.500 m. The results, summarized in Table II in the Appendix, show that the average travel distance is 3.516 m, the standard deviation is 0.0031 m, and the maximum error is 0.023 m; these findings are considered sufficiently accurate for use in this experiment.

### C. Non-human-like Appearance

Fig. 3(a) shows the robot's appearance under the Non-human-like condition. While maintaining the same overall size as in the Human-like condition, the robot was equipped with a head devoid of human-like features, and dummy

cameras were placed at the same eye positions as the human-like robot. The upper body, lower body, and mobile base were left uncovered, leaving the internal mechanisms exposed. Only the head shape, presence or absence of blinking and facial expressions, and the clothing differed in the two tested conditions; all other movements, orientations, and motion profiles explained in Section II-B were identical to those in the Human-like condition.

### D. Human-like Appearance

Fig. 3(b) shows the robot's appearance under the Human-like condition. The head was equipped with an android head unit [13] featuring human-like characteristics, while the upper body, lower body, and mobile base were covered with human clothing. The android was given a feminine appearance for two reasons: (I) because skirts are ideal for naturally concealing the legs of the robot, and (II) to maintain a consistent gender impression. Fig. 4 shows the robot's facial expression during movement. While in motion, the eyelids were actuated to produce a blink lasting 0.3 s every 2.0 s, and the cheek-lift and lip-corner were actuated to maintain a smiling expression. The body movements are described in Section II-B.

## III. METHODS

This section outlines the method for quantifying the personal space perceived by participants in response to both the android used in the Human-like condition and the robot used in the Non-human-like condition. This section also details the procedure for evaluating participants' impressions of each robot.

### A. Participants

According to Hecht et al. [6], personal space size is influenced by gender, while Hall [3] reported that it is also shaped by cultural factors. In this experiment, conducted under the Human-like condition, a feminine robot appearance was used, as described in Section II-D. Therefore, to control for potential effects of gender and culture, only Japanese male participants aged 18 years or older were recruited. Twenty-three students from the University of Electro-Communications took part in the study. All participants were Japanese males aged 19 – 29 years, with 12 assigned to the Non-human-like condition and 11 to the Human-like condition. Each participant received a cash voucher valued at 1000 JPY as a token of appreciation.

Participants were excluded when the robot failed to stop upon the button press intended to halt its approach, when it approached them from the same direction twice instead of once during the eight-direction sequence, or when their questionnaire responses were incomplete. As a result, data from nine participants in the Non-human-like condition and 10 participants in the Human-like condition were used for analysis.

### B. Materials

Fig. 5(a) shows the experimental setup. As illustrated in Fig. 5(a), 0° was defined as the orientation in which the participant and the robot directly faced each other. The participant was subsequently rotated in 45° counterclockwise increments so that, within the participant's frame of reference, the robot approached from eight directions (0°, 45°, ⋯, 315°). For each direction, the participant halted the approaching robot by pressing a handheld button upon perceiving discomfort, and the corresponding distance was recorded as the personal space distance. The personal space, defined as the area individuals maintain around themselves into which intrusion by others causes discomfort [14], was determined for each participant by compiling the distances for all angles.

In this study, participants' eye levels were standardized to reduce the effects of eye level differences when they faced the robot. Participants sat in a chair, and their eye levels were adjusted to 1.3 m. This height was selected because it fell within the adjustable range of the chair and allowed most male participants to align their gaze with the robot.

Two types of robots—human-like and non-human-like—were created by modifying the same robot's head, hands, and clothing while using identical walking motions. This modification was implemented between the first and second halves of the experimental period. The robot's movement was designed to begin with acceleration, continue at a constant speed (0.34 m/s), and end with deceleration. At this time, an experiment assistant was present to intervene in cases where the robot was unable to decelerate in time. The experiment was conducted within the space and positional arrangement between the robot and the participant, shown in Fig. 5(b).

In the experiment, a questionnaire was provided to assess participants' likability toward the robot. The Japanese version of the Godspeed questionnaire [15] was used, focusing only on the likability subscale. This questionnaire consists of five pairs of opposing adjectives. Participants were asked to indicate which impression they perceived was closer by selecting a score value from 1 to 5, with higher values indicating more positive impressions. The average of the five values was used as a likability score. The adjective pairs employed were dislike–like, unfriendly–friendly, unkind–kind, unpleasant–pleasant, and awful–nice, which were translated into Japanese and incorporated into the questionnaire.

### C. Procedures

The experimental procedure was as follows. Each participant was first seated in a chair and adjusted the chair height so that their eye level was 1.3 m. After this adjustment, a handheld button was provided to each participant. The robot then approached from eight angular directions relative to the participant, ranging from $0^\circ$ to $315^\circ$ in $45^\circ$ increments. Each approach direction was assigned a corresponding number from 1 to 8.

In the first trial, the experimenter indicated the number corresponding to the first randomized angle. The participant then rotated the chair accordingly so that both feet straddled

(a) Overview of the experimental scene. The participant's role is portrayed by one of the authors by holding a handheld switch that is used to stop the approaching robot. The robot shown is in the Human-like condition.

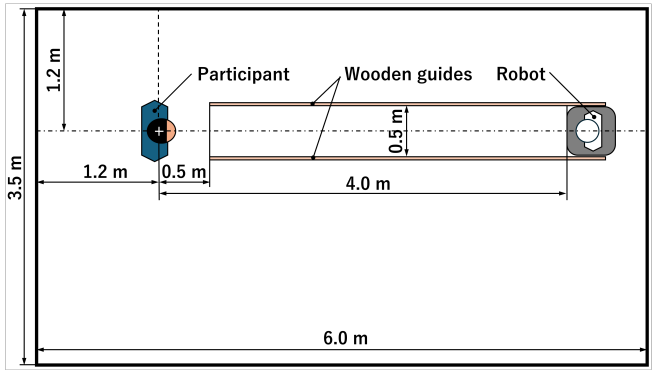


(b) Top-down schematic view of the experimental site. Wooden guides were fixed to the floor along both sides of the robot's path to constrain its movement direction.

Fig. 5: Experimental setup.

the line marked with that number, facing the instructed angle. Subsequently, the participant was asked to turn their upper body to face the direction from which the robot would approach, without rotating the chair.

Upon receiving the experimenter's cue, the robot initiated a movement from a starting distance of 4.0 m. It accelerated smoothly until reaching a constant velocity of 0.34 m/s, maintaining a straight trajectory toward the participant. During the approach, the robot's head was directed toward the participant, while its eyes remained fixed in a neutral, forward-facing position, avoiding any attempt to establish eye contact. If the participant did not intervene, the robot subsequently decelerated and stopped at a distance of 0.5 m.

During the robot's approach, the participant was instructed to press the button at the instant at which the robot's presence was perceived as uncomfortable for a conversation. After stopping the robot, the participant turned to face a direction $180^\circ$ away from the robot (i.e., in a direction where the robot was not visible), and the robot was moved back to its starting position.

This procedure was repeated once for each of the eight approach angles. The order of the numbers indicated by the experimenter was randomly determined in advance for each subject.

Finally, the participants rated their likability toward the robot in the questionnaire and provided comments in a free-response section.

### D. Ethical Considerations

The Ethics Committee of the University of Electro-Communications approved the study protocol (No. H25016).

All participants provided written informed consent prior to participation in the experiment.

## IV. Results

The plot of the measured distance is shown in Fig. 6(a), and the median-based distance distributions—used to minimize the strong influence of outliers resulting from the small sample size—are illustrated in Fig. 6(b). Statistical comparisons were performed using the Mann–Whitney U test. The table in Fig. 6(c) presents the test statistics ($U$, $p$-values, and median distances) for both conditions across all directions. In the table, $M_{NH}$ represents the median for the Non-human-like condition, and $M_H$ represents the median for the Human-like condition. The results indicate that the personal space perceived by participants tended to form a shape close to a regular octagon under the Human-like condition, with greater distances observed in the rear direction. In contrast, under the Non-human-like condition, the rear personal space tended to be smaller. However, statistical analysis using the Mann–Whitney U test revealed no significant differences in distance as a function of angle in any direction.

Fig. 7 shows likability scores for each robot condition. The results indicate that the Human-like condition had a higher median and greater variance in likability compared with the Non-human-like condition. However, a statistical comparison using the Mann–Whitney U test revealed no significant difference in likability score between the two conditions ($U = 40.0$, $p = 0.712$).

The relationships between likability score and the size of personal space are shown in Fig. 8(a). As shown in the figure, likability score was the average value of participants' responses to the five Likert-scale questions, and the corresponding distance was derived by converting the area of the octagonal region of the personal space into the radius of a circumscribed circle of a regular octagon. The Spearman's rank correlation coefficient was used to test the relationship between likability and personal space. Hereafter, the correlation in the Non-human-like condition is denoted as $r_{NH}$, the correlation in the Human-like condition is denoted as $r_H$, and the correlation for all participants is denoted as $r_{all}$. The results revealed a significantly strong negative correlation between the two variables ($r_{all} = -0.777$, $p < 0.05$). Furthermore, significant negative correlations were observed in both conditions; however, the correlation was stronger in the Non-human-like condition ($r_{NH} = -0.817$, $p < 0.05$) than in the Human-like condition ($r_H = -0.781$, $p < 0.05$).

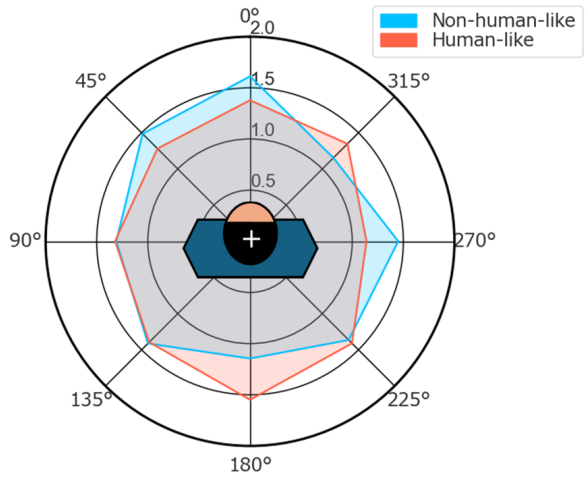


(a) Polar plot of median personal space distances across a range of approach angles for the Non-human-like and Human-like conditions.

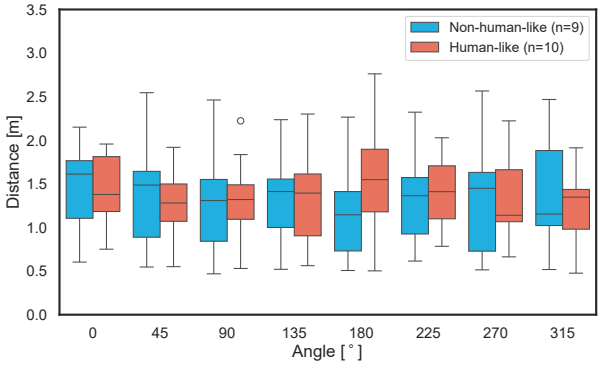


(b) Box plots showing personal space distance distributions by angle. (The box spans the first to third quartiles (Q1–Q3), with its height representing the interquartile range (IQR). The line inside the box indicates the median. Whiskers extend to data points within 1.5 × IQR from Q1 and Q3, and any observations beyond this range are plotted as outliers.)

(c) Results of the Mann–Whitney U test.

| Angle [°] | $M_{NH}$ [m] | $M_H$ [m] | $U$ | $p$ |
|---|---|---|---|---|
| 0 | 1.612 | 1.379 | 47.0 | 0.903 |
| 45 | 1.486 | 1.281 | 48.0 | 0.838 |
| 90 | 1.309 | 1.320 | 43.0 | 0.903 |
| 135 | 1.412 | 1.395 | 44.0 | 0.967 |
| 180 | 1.146 | 1.549 | 32.0 | 0.307 |
| 225 | 1.365 | 1.411 | 38.0 | 0.596 |
| 270 | 1.450 | 1.140 | 44.0 | 0.967 |
| 315 | 1.154 | 1.348 | 47.0 | 0.903 |

Fig. 6: Personal space results.

Additionally, Fig. 8(b) and 8(c) illustrate the relationships between likability score and the distance in the front (0°) and rear (180°) directions, respectively. Both yielded significant moderate negative correlations (front: $r = -0.660$, $p < 0.05$; rear: $r = -0.611$, $p < 0.05$). Furthermore, in the front direction, a significant negative correlation was observed between likability score and the Non-human-like condition

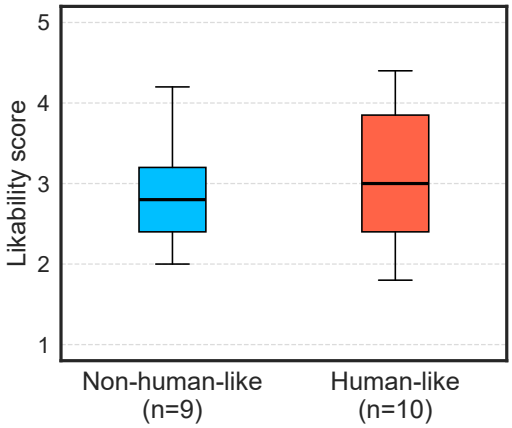


Fig. 7: Distribution of likability scores under the Non-human-like and Human-like conditions. Each score represents the average of the five Godspeed likability subscale items.

($r_{NH} = -0.767$, $p < 0.05$), while in the rear direction, a significant negative correlation was observed between likability score and the Human-like condition ($r_H = -0.738$, $p < 0.05$).

## V. DISCUSSION

In this study, we investigated how robot appearance—specifically human-like and non-human-like designs—influences personal space during direct robotic approaches, and how this relates to perceived likability. No significant personal space distance differences were found between the two appearance conditions (Fig. 6), and likability scores did not differ significantly between the two conditions (Fig. 7), indicating that the change in appearance alone did not affect participants' evaluations. However, a negative correlation was typically observed between likability score and personal space distance (Fig. 8), even though its strength varied according to the approach direction and condition. In other words, participants who rated the robot more favorably tended to allow it to approach them more closely, regardless of its appearance. This finding is consistent with previous studies [6] showing that feelings of likability in interpersonal interaction are reflected in physical distance preferences.

Regarding the overall shape of personal space, no statistically significant differences were observed between the two conditions (Fig. 6(b)). However, Fig. 6(a) revealed distinct spatial patterns that merit further investigation. Hayduk [16] reported that human–human personal space tends to be larger in the frontal direction. Interestingly, the spatial distribution observed in the Non-human-like condition appeared consistent with this interpersonal baseline. This finding suggests that, because the Non-human-like robot possessed an anthropomorphic structure (e.g., a defined head and torso) despite its mechanical exterior, participants may have subconsciously applied human-based proxemic rules similar to those described by Hayduk. In contrast, the Human-like condition displayed a different spatial profile, with a noticeably larger rear space. This deviation may reflect heightened vigilance

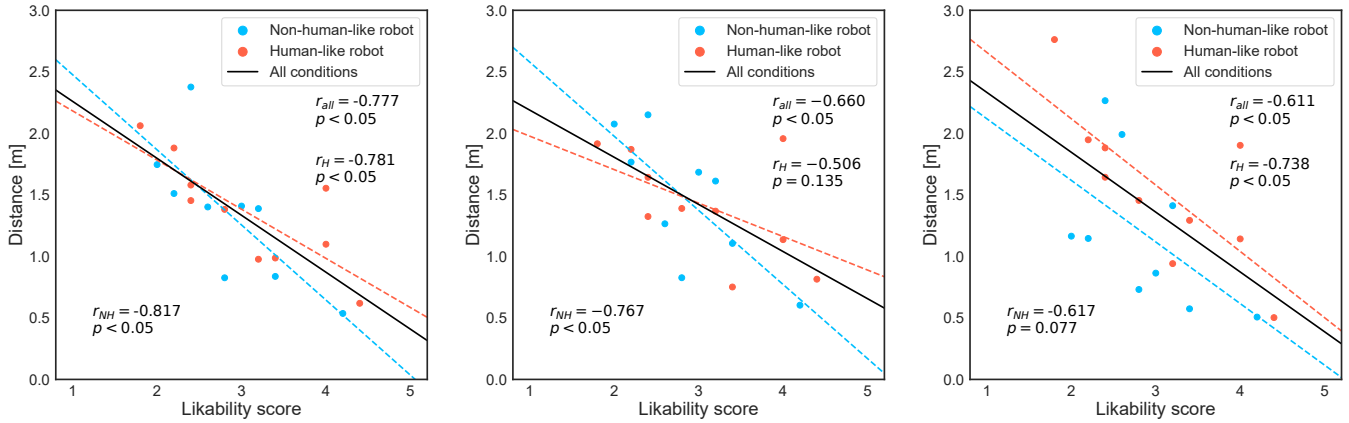


(a) Average distance plot as a function of likability.

(b) Front direction (0°) distance plot as a function of likability.

(c) Rear direction (180°) distance plot as a function of likability.

Fig. 8: Relationships between likability and personal space distance in the Non-human-like and Human-like conditions.

caused by subtle nonhuman cues, such as mechanical motion patterns or the absence of mutual gaze. These interpretations remain speculative and require empirical validation in future studies.

In this experiment, the Human-like condition was defined by the robot being equipped with a head and hands designed to resemble human morphology and covered with clothing. Conversely, the Non-human-like condition was characterized by a head intentionally designed to minimize human resemblance, aside from its basic shape, and an exposed mechanical body structure. However, this study did not confirm whether participants actually perceived these two configurations as differing in human-likeness. Future research should therefore include explicit assessments of perceived human-likeness and explore a broader range of appearance variants—such as designs with concealed neck mechanisms or non-anthropomorphic platforms (e.g., cylindrical or box-shaped robots)—to elucidate how visual appearance influences personal-space regulation.

Furthermore, because the primary objective was to isolate the effect of appearance, all non-appearance parameters, including motion, were kept constant across conditions. However, motion itself is a salient determinant of perceived human-likeness. Future work should thus investigate the interaction between appearance and motion in shaping personal-space judgments, incorporating comparisons with stationary robots and diverse movement types.

The instruction to determine the point at which the robot became "uncomfortable for a conversation" was designed to simulate realistic interaction scenarios, such as service or delivery robots approaching users for brief verbal exchanges. However, task framing is known to influence spatial judgments. Future studies should therefore systematically compare conversational, safety-oriented, and neutral framings to clarify how contextual goals affect personal-space evaluation.

Additionally, a potential concern is the influence of participants' tension or habituation over repeated trials. Although the eight approach directions were randomized to minimize such effects, personal-space distances were further analyzed as a function of trial order (see Fig. 9 in Appendix II). The results showed no consistent trends, indicating that any effects of initial tension or habituation were minimal and unlikely to have confounded the main findings.

Although meaningful relationships were identified, the statistical power of the analyses was constrained by the relatively small sample sizes in each appearance condition (n = 9 and n = 10). The generalizability of the findings was further limited by the demographic homogeneity of the participants—Japanese male university students aged 19–29 years—and by the use of a child-sized android with a feminine appearance. These design choices were intended to minimize variability arising from gender and cultural factors [6], yet they inevitably restricted broader applicability across populations and robot morphologies. Additionally, only a single set of motion parameters was evaluated, and other socially relevant cues, such as speech and gaze, were not manipulated, despite their well-documented impact on interpersonal distance. The absence of high-DOF, human-like gait further limits the interpretation of locomotor human-likeness effects.

Future research should therefore simultaneously manipulate appearance, motion, and communicative behaviors—including facial expressions, gaze cues, and vocal signals—to investigate their combined influence on personal-space regulation. Incorporating more human-like locomotion derived from recorded human gait and realized through coordinated multi-DOF control would enable systematic exploration of how movement dynamics shape perceived human-likeness and likability. Such investigations will advance the development of androids and service robots capable of socially adaptive and context-sensitive interactions.

## VI. CONCLUSIONS

To the best of our knowledge, this study conducted the first systematic examination of personal space in the context of the direct approach of a highly human-like android. An

TABLE II: Measured Travel Distances in 10 Trials (Target: 3.500 m)

| Trial Number | Distance $L$ [m] |
|---|---|
| 1 | 3.517 |
| 2 | 3.523 |
| 3 | 3.519 |
| 4 | 3.514 |
| 5 | 3.514 |
| 6 | 3.512 |
| 7 | 3.518 |
| 8 | 3.515 |
| 9 | 3.514 |
| 10 | 3.516 |

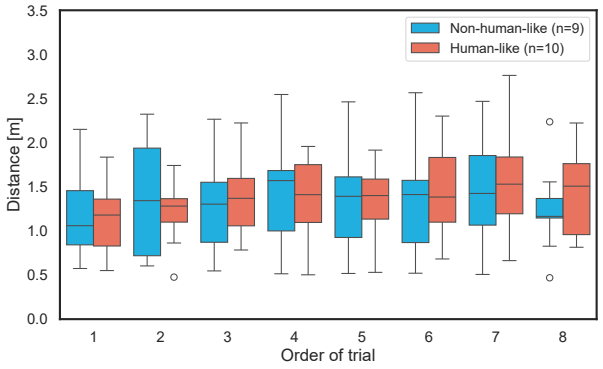


Fig. 9: Personal space distance as a function of trial order (1–8).

experimental system was developed using a mobile android platform, enabling measurements of personal space under human-like and non-human-like appearance conditions. In the Human-like condition, the personal space shape was almost circular with a radius of approximately 1.35 m, whereas in the Non-human-like condition, the personal space shape exhibited a tendency toward larger front and smaller rear parts. No significant differences in size were found between conditions, and likability scores did not differ. Nonetheless, a negative correlation was observed between likability score and personal space distance, indicating that participants who evaluated the robot more positively tended to allow it to approach them more closely. These findings provide baseline data for understanding interpersonal distance regulation in human–robot interactions, particularly in relation to robotic appearance, and demonstrate that perceived likability correlates with preferred interpersonal distance. Future research should investigate how appearance, motion, and communicative behaviors—such as facial expressions, gaze, and vocal cues—jointly shape personal-space regulation.

## Appendix I
## Verification of Encoder Distance Accuracy

Table II lists the results of the wheel encoder accuracy verification. The data were obtained from 10 trials where the robot traveled 3.500 m, and the measured distances were compared with values from tape measurements.

## Appendix II
## Personal Space as a Function of Trial Order

Fig. 9 illustrates the distribution of personal distance values recorded for each trial order. No consistent or systematic trend was observed across the data.

## References


[1] N. Gasteiger, M. Hellou, and H. Ahn, "Deploying social robots in museum settings: A quasi-systematic review exploring purpose and acceptability," *International Journal of Advanced Robotic Systems*, vol. 18, pp. 1–13, 2021.

[2] M. Zimmerman, S. Bagchi, J. Marvel, and V. Nguyen, "An analysis of metrics and methods in research from human-robot interaction conferences, 2015–2021," in *2022 17th ACM/IEEE International Conference on Human-Robot Interaction (HRI)*, 2022, pp. 644–648.

[3] E. T. Hall, *The hidden dimension*. Anchor Books, 1990.

[4] L. Takayama and C. Pantofaru, "Influences on proxemic behaviors in human-robot interaction," in *2009 IEEE/RSJ International Conference on Intelligent Robots and Systems*, 2009, pp. 5495–5502.

[5] M. Walters, K. Dautenhahn, R. te Boekhorst, K. L. Koay, C. Kaouri, S. Woods, C. Nehaniv, D. Lee, and I. Werry, "The influence of subjects' personality traits on personal spatial zones in a human-robot interaction experiment," in *ROMAN 2005. IEEE International Workshop on Robot and Human Interactive Communication, 2005.*, 2005, pp. 347–352.

[6] H. Hecht, R. Welsch, J. Viehoff, and M. Longo, "The shape of personal space," *Acta Psychologica*, vol. 193, 2018.

[7] H. Lehmann, A. Rojik, and M. Hoffmann, "Should a small robot have a small personal space? investigating personal spatial zones and proxemic behavior in human-robot interaction," 2020.

[8] M. Joosse, M. Lohse, N. van Berkel, A. Sardar, and V. Evers, "Making appearances: How robots should approach people," *ACM Transactions on Human-Robot Interaction*, vol. 10, 2020.

[9] E. Torta and R. Cuijpers, "Design of a parametric model of personal space for robotic social navigation," *International Journal of Social Robotics*, vol. 5, 2013.

[10] K. Kaneko, F. Kanehiro, M. Morisawa, K. Miura, S. Nakaoka, and S. Kajita, "Cybernetic human HRP-4C," in *2009 9th IEEE-RAS International Conference on Humanoid Robots*, 2009, pp. 7–14.

[11] H. S. Ahn, D.-W. Lee, D. Choi, D.-Y. Lee, M. Hur, and H. Lee, "Appropriate emotions for facial expressions of 33-dofs android head EveR-4 H33," in *2012 IEEE RO-MAN: The 21st IEEE International Symposium on Robot and Human Interactive Communication*, 2012, pp. 1115–1120.

[12] Y. Nakata, S. Yagi, S. Yu, Y. Wang, N. Ise, Y. Nakamura, and H. Ishiguro, "Development of 'ibuki' an electrically actuated childlike android with mobility and its potential in the future society," *Robotica*, vol. 40, no. 4, pp. 933–950, 2022.

[13] M. Nakajima, K. Shinkawa, and Y. Nakata, "Development of the lifelike head unit for a humanoid cybernetic avatar 'Yui' and its operation interface," *IEEE Access*, vol. 12, pp. 23 930–23 942, 2024.

[14] D. Kennedy, J. Gläscher, J. Tyszka, and R. Adolphs, "Personal space regulation by the human amygdala," *Nature Neuroscience*, vol. 12, pp. 1226–1227, 2009.

[15] C. Bartneck, *Godspeed Questionnaire Series: Translations and Usage*. Cham: Springer International Publishing, 2023, pp. 1–35.

[16] L. A. Hayduk, "The shape of personal space: An experimental investigation." *Canadian Journal of Behavioural Science*, vol. 13, no. 1, pp. 87–93, 1981.